Supporting Information**:**

On the origin of the Norwegian lemming

Vendela K. Lagerholm, Edson Sandoval-Castellanos, Dorothee Ehrich, Natalia I. Abramson, Adam Nadachowski, Daniela C. Kalthoff, Mietje Germonpré, Anders Angerbjörn, John R. Stewart, Love Dalén

Contents

SI Materials and methods

DNA extraction and amplification

Late Pleistocene *Lemmus* spp. mandibles were sampled using a Multitool drill to recover approximately 30 mg of bone powder. DNA was subsequently extracted from the bone powder using the modified version of protocol C in Yang *et al*. (1998), where SDS in the lysis buffer was replaced with 1M UREA, and concentration of the post-lysis supernatant was done using 30K MWCO Vivaspin filters (Sartorius) before purification on silica columns. DNA from the Holocene Scandinavian samples was extracted from completely grinded bone material using Qiagen's QIAamp Tissue kit as described in Fernández *et al*. (2006).

For both the Late Pleistocene and the modern material, 168 bp part of the control region (CR) and 352 bp part of the cytochrome *b* (cyt *b*) gene was amplified in two and three overlapping fragments respectively, using genus specific primer pairs developed for this study (Table S3). Polymerase chain reactions (PCRs) were carried out in 25 µl volumes, each containing 1 X PCR buffer, 2.5 mM $MgCl_2$, 0.1mg/ml BSA, 0.2 mM of each dNTP, 0.4 U Hotstar Taq (Qiagen), 0.2 µM of each primer and 2 µl of extracted DNA. The thermal profile included an initial 10 min denaturation step at 95 °C, followed by either 55 (Pleistocene material) or 40 (modern material) cycles of 30 sec at 94 °C, 30 sec at 48 °C (CR) or 52 °C (cyt *b*), 30 sec at 72 °C, as well as a final 7 min elongation step at 72 °C. After PCR products had been cleaned using Exo-FAP, with 1 part Exonuclease I (20 U/µl) and 4 parts FastAP Alkaline Phosphatase (1 U/µl) (Fermentas), both forward and reverse strands were sequenced using an ABI 3130xl (Applied Biosystems).

For the analyses of the Holocene Scandinavian samples, two genus-specific primer pairs were developed to target the mitochondrial CR (96 bp) and cyt *b* gene (76 bp) (Table S3). PCRs were set up according to the procedures described in Fernández *et al*. (2006), with annealing temperatures set to 52 °C (CR) and 55 °C (cyt *b*).

Bayesian coalescent simulations

Background and model design

Approximate Bayesian Computation coupled with coalescent simulations consists in getting a large number of simulations of a model of the system governing the properties of the observed data, with parameter values randomly generated from prior distributions. A rejection algorithm is subsequently applied, so that the simulated data sets that are similar enough to the observed data (evaluated using summary statistics) are retained and their associated parameter values are considered a sample from the posterior distribution conditional to the observed data set (Beaumont *et al.* 2002). Finally, the obtained posterior distributions can be employed for statistical inference, whilst acceptance ratios (Bayes factors) allow hypothesis testing (Bertorelle *et al.* 2010).

We used the program Bayesian Serial SimCoal (Anderson *et al.* 2005; Excoffier *et al.* 2000) to run coalescent simulations (Fig. S1), including 4 million simulations for optimisation/sequential steps, 2 million simulations for obtaining Bayes Factors for model comparisons (hypothesis contrast), 20 million simulations for punctual estimation of the parameters of interest, and 1.6 million simulations for a cross-validation test using pseudo-observed datasets (PODs). The PODs analysis is a verification method that establishes the statistical properties of the analysis, and its power and robustness (i.e. the sensibility of the results to incorrect parameters or model choice). In this analysis, a correct scenario choice was when a scenario got more support than the alternative(s). After pilot simulations had been carried out to identify key parameters and adjust the model design, as well as for selecting proper summary statistics

(SuS), a sequential algorithm with only one cycle was used to run additional optimisation simulations in order to set the parameters and fit the distributions according to the obtained posteriors (but using wider variances) to be used as priors in the final simulations (Bertorelle *et al.* 2010; Lopes *et al.* 2009). Post simulation analyses were made in a custom software written in the programming language Fortran 95 (available upon request), using the integrated development environment Microsoft Visual Studio 2010 with the Intel Fortran Compiler XE 12.1 extension.

Instead of using a composite distance as thresholds for the SuS, we performed rejection on the basis of a vector of distances, one for each SuS, with the most relevant SuS being the most constrained (Table S2). The former approach to use a composite distance is set to accept a pre-defined proportion of the simulations (e.g. 1%) which are closest to the observed data. This means that it is possible to accept simulations with extreme values as long as the composite distance is low. Our method of using a vector of distances requires additional analyses and effort directed to find the values that produce a target number of accepted simulations, where all SuS values needs to be within the acceptance interval. This approach provides more control on the rejection procedure and avoids the acceptance of simulations with extreme values for key SuS.

The post-simulation analyses included recovery of histograms and descriptive statistics from the accepted SuS. Due to our rejection approach for the SuS, as well as the fact that such a large number of simulations was required that they had to be divided and run in different groups, the analysis procedure was incompatible with regression. Simple rejection was therefore employed instead. However, according to Lopes and Beaumont (2010) this should not affect the conclusions, since results from both regressed and non-regressed analyses tend to converge when the number of simulations is large.

Box S1 Input data set for Bayesian Serial SimCoal. Values shown here correspond to the glacial survival hypothesis in scenario 2 and a mutation rate of 50 % Myr^{-1}, using the partial data set. Notes were added after a double slash (//).

```
4 populations with ancient DNA
// Ne priors (in this case Gamma distribution with parameters of shape and scale)
{G:1.25,215000}   // Scandinavia
{G:1,75,25000}    // Glacial England
{G:3.9,25000}     // Glacial continental Europe
{G:1.15,65000}    // Siberia
//Samples sizes: # samples, age, deme, statistical group
15     // # of sampling groups.
//Columns are: Sample size, age (or prior -Normal distrib. μ,σ-), population & stat. group
17 0                0 0  //      1.Sweden (modern Lemmus lemmus)
2  {N:2800,300}     0 0  //      1.Norway
4  {N:7100,400}     0 0  //      1.Norway
2  {N:8100,400}     0 0  //      1.Norway
1  {N:11400,100}    1 1  //      2.Eng
4  {N:12300,100}    1 1  //      2.Eng
1  {N:12400,100}    1 1  //      2.Eng
5  {N:28600,5000}   2 2  //      3.Rus(U)
1  {N:28600,200}    2 2  //      3.Rus(U)
5  {N:36000,4000}   2 2  //      3.Rus(Pl)
2  {N:13300,200}    2 2  //      3.Pol
1  {N:28400,4000}   2 2  //      3.Ger
1  {N:46900,500}    2 2  //      3.Bel
2  {N:47900,500}    2 2  //      3.Bel
10 0                3 3  //      4.Sib (modern Lemmus sibiricus)
//Growth rates of each population (negative means pop expansion)
{U:-0.001,0.0}  //Only an expansion of the Scandinavian population was considered
0
0
0
//Number of migration matrices; 0 := No migration
0
//Historical events: time, source, sink, migrants, new deme size, new growth rate, new mig
//matrix
4 historical events  //First column is the time with uniform priors with indicated bounds
11500                 0 0 1 1 0 0 // The growth starts
{U:12000,120000}   0 1 1 1 0 0 // The split Scandinavia - England
{U:50000,200000}   3 2 1 1 0 0 // The split Siberia - Cont. Europe
{U:120000,200000} 1 2 1 1 0 0 // The split ScandinaviaEngland - Cont. Europe
//Mutation rate per generation for the whole sequence
0.000127 //  = 50% Myr^-1
//Number of loci
172
//Data type set to DNA. Second term is the transition bias
DNA 0.8787 //Transition/transversion is the prob. of a mutation being A<->G or C<->T
//Gamma parameter
0.150 5
```

Results and discussion

The differences between the distributions of the SuS from the simulations of the two hypothesised scenarios illustrated the behaviour of the SuS, and their usefulness in distinguishing between the proposed hypotheses. In summary, the SuS that can be defined as genetic variability descriptors (HapTypes, SegSites and PairDiff) had similar distributions for the two scenarios, and therefore did not help to discriminate between them. However, they served as fine tuning and optimisation of the simulations, by adjusting parameters and settings so that the final simulations better fitted the observed data, whilst increasing the probability of acceptance of simulations for a given threshold distance. The SuS that showed well differentiated distributions between scenarios, and therefore were crucial for the inference, were the pairwise differences between populations and the F_{ST} between populations (Fig. S4).

Comparisons of the SuS distributions with and without rejection showed that the rejection had a significant effect in changing the distributions associated with the simulations, whether they were parameters or SuS (Fig. S5). Not only did the election of the employed SuS follow a dedicated analysis, but also the election of the acceptance thresholds for each SuS. Thus, the "variability descriptor" statistics were medium constrained, while the F_{ST} and pairwise differences between populations where constrained to the maximum possible. The thresholds for the SuS associated with populations that were not directly the target of the inference (pop. 3 and 4: continental glacial Europe and *Lemmus sibiricus*) were more relaxed than the rest (Table S2).

SI Tables

Table S1 All samples included in the study. Values in parenthesis within the Site column corresponds to the number of successful samples (left) out of the total number of samples analysed (right). Lab, GenBank, and OxA (from The Oxford Radiocarbon Accelerator Unit) numbers, as well as the group number assigned in the Bayesian coalescent simulations (Sim), are shown for all successful samples included in the data analyses. Hap#p and Hap#c corresponds to the Haplotype IDs shown in the networks for the partial and the complete data sets. Ages of dated samples are reported in both radiocarbon years (C14 age) and calendar years before present (age BP). Additionally, the estimated ages obtained from tip sampling in BEAST are shown for the Studennaya samples. Modern Scandinavia and NW Russia corresponds to the species *Lemmus lemmus* and *Lemmus sibiricus*, respectively.

Site (n)	Region	Lat itude	Longitude	Lab	GenBank	C14 age	OxA	age BP	Hap#p	Hapl#c	Sim
Late Pleistocene Europe											
Merlin's Cave (1/5)	England	50°40'07"N	04°45'35"W	V327	JX483914	failed		~11,4 k [1]	19	17	2
Bridged Pot (5/5)	England	51°14'03"N	02°40'53"W	V042	JX483909	10,400±50	(OxA-25376)	12,3 k	20	18	2
				V043	JX483910	-		~12,3 k [2]	19	17	2
				V044	JX483911	10,460±50	(OxA-25377)	12,4 k	21	20	2
				V045	JX483912	-		~12,3 k [2]	19	17	2
				V046	JX483913	-		~12,3 k [2]	19	19	2
Caverne Marie Jeanne (3/6)	Belgium	50°13'N	04°48'E	V003	JX483915	43,200± 2000	(OxA-25374)	46,9 k	34	33	3
				V005	JX483916	45,500± 2700	(OxA-25375)	47,9 k	32	30	3
				V006	JX483917	-		~47,9 k [3]	33	34	3
Walou Cave (0/5)	Belgium	50°35'29"N	05°41'46"E	-		-					
Neandertal (1/5)	Germany	51°13'36"N	06°56'49"E	V119	JX483918	failed		28,4 k [4]	35	35	3
Deszczowa Cave (0/1)	Poland	50°34'N	19°31'E	-		-					
Krucza Skala (2/2)	Poland	50°33'41"N	19°34'10"E	V048	JX483919	failed		~13,3 k [5]	30	32	3
				V049	JX483920	-		~13,3 k [5]	31	31	3
Pushkari (0/7)	Russian plains	52°12'02"N	33°17'30"E	-		-					
Yudinovo (0/1)	Russian plains	52°40'14"N	33°15'45"E	-		-					
Betovo (5/8)	Russian plains	53°20'39"N	34°01'02"E	V088	JX483927	failed		~41,2 k [6]	28	28	3
				V089	JX483928	-		~41,2 k [6]	29	29	3
				V090	JX483929	-		~41,2 k [6]	29	29	3
				V091	JX483930	failed		~41,2 k [6]	27	25	3
				V093	JX483931	-		~41,2 k [6]	27	26	3
Studennaya (6/9)	Ural mts	59°40'N	60°00'E	V050	JX483921	failed		~28,6 k [7] ~33,1; 29,8; 24,0 k	22	21	3
				V052	JX483922	-		~28,6 k [7] ~27,9; 27,0; 27,4 k	25	24	3
				V054	JX483923	-		~28,6 k [7] ~32,3; 33,9; 34,6 k	24	23	3
				V056	JX483924	-		~28,6 k [7] ~31,0; 33,6; 35,6 k	26	27	3
				V057	JX483925	-		~28,6 k [7] ~32,3; 33,9; 34,5 k	24	23	3
				V058	JX483926	23,780± 200	(OxA-25378)	28,6 k ~32,9; 35,2; 35,8 k	23	22	3

Holocene Scandinavia										
Sirijorda Cave (8/27)	Norway	65°32'03"N	13°09'21"E	a1	JX483932	-	~2,8 k [8]	1	-	1
				a2	JX483933	-	~2,8 k [8]	1	-	1
				a3	JX483934	-	~7,1 k [8]	6	-	1
				a4	JX483935	-	~7,1 k [8]	5	-	1
				a6	JX483936	-	~8,1 k [8]	18	-	1
				a12	JX483937	-	~7,1 k [8]	7	-	1
				a20	JX483938	-	~8,1 k [8]	1	-	1
				a26	JX483939	-	~7,1 k [8]	1	-	1
Modern Scandinavia										
Jämtland (3/3)	Sweden	62°50'N	12°20'E	V245	JX483892			9	10	1
				V258	JX483901			9	10	1
				V261	JX483902			4	5	1
Jämtl./Västerb (2/2)	Sweden	64°50'N	15°05'E	V252	JX483898			8	2	1
				V253	JX483899			9	10	1
Västerbotten (3/3)	Sweden	65°54'N	15°15'E	V246	JX483893			1	1	1
				V247	JX483894			4	5	1
				V254	JX483900			7	4	1
Sarek, Norrbotten (2/2)	Sweden	67°10'N	17°44'E	V287	JX483907			10	9	1
				V291	JX483908			2	8	1
Padjelanta, Norrbotten (2/2)	Sweden	67°25'N	16°50'E	V249	JX483896			7	4	1
				V250	JX483897			1	1	1
Kebnekaise, Norrbotten (2/2)	Sweden	67°54'N	18°36'E	V285	JX483905			3	6	1
				V286	JX483906			7	4	1
Abisko, Norrbotten (3/3)	Sweden	68°20'N	18°49'E	V248	JX483895			10	7	1
				V265	JX483903			10	9	1
				V266	JX483904			11	3	1
Modern NW Russia										
Derevnya (2/2)	Russia	64°25'N	51°10'E	V323	JX483889			17	16	4
				V324	JX483890			17	16	4
Pechora (1/2)	Russia	65° 08'N	57°13'E	V325	JX483891			14	13	4
Amderma (7/7)	Russia	69°45'N	61°40'E	V316	JX483882			14	13	4
				V317	JX483883			12	11	4
				V318	JX483884			14	13	4
				V319	JX483885			13	12	4
				V320	JX483886			14	13	4
				V321	JX483887			16	15	4
				V322	JX483888			15	14	4

[1] Mean of published dates from the same site (Ramsey *et al.* 2002). [2] Mean of our dates from the same site. [3] Based on the date of V005 from the same layer. [4] Mean of previous dates from the same site (Schmitz pers.comm). [5] Based on a published date from the same layer (Bochenski & Tomek 2004). [6] Based on a published date from the same site (Abramson *et al.* 2004). [7] Based on the date of V058 from the same site. [8] Mean of published dates from the same layers (Østbye *et al.* 2006).

Table S2 Summary statistics employed in the Bayesian coalescent simulations. The empirical (observed) values and distance thresholds used for rejection are here shown for the partial data set analyses. Population numbers correspond to the groups listed in Table S1.

Short Name	Brief description	Observed	Acceptance radius		
			11.7 %	30 %	50 %
HapTypes1	Number of haplotypes in pop. 1	12.00	8.10	6.75	6.38
SegSites1	Number of segregating sites in pop. 1	21.00	13.50	11.25	10.63
PairDiffs1	Average no. of pairwise differences in pop. 1	4.37	3.15	2.63	2.48
HapTypes2	Number of haplotypes in pop. 2	3.00	1.80	1.50	1.42
SegSites2	Number of segregating sites in pop. 2	7.00	7.20	6.00	5.67
PairDiffs2	Average no. of pairwise differences in pop. 2	6.05	3.60	3.00	2.84
HapTypes3	Number of haplotypes in pop. 3	14.00	4.50	3.75	3.54
SegSites3	Number of segregating sites in pop. 3	28.00	13.50	11.25	10.63
PairDiffs3	Average no. of pairwise differences in pop. 3	20.69	13.50	11.25	10.63
HapTypes4	Number of haplotypes in pop. 4	6.00	3.60	3.00	2.84
SegSites4	Number of segregating sites in pop. 4	9.00	18.00	15.00	14.18
PairDiffs4	Average no. of pairwise differences in pop. 4	2.93	13.50	11.25	10.63
PairDiffs1vs2	Average no. of pairwise differences between pop. 1 & pop. 2	15.66	6.75	5.63	5.32
Fst1vs2	F_{ST} between pop. 1 & pop. 2	0.69	0.32	0.26	0.25
PairDiffs1vs3	Average no. of pairwise differences between pop. 1 & pop. 3	23.03	25.20	21.00	19.85
Fst1vs3	F_{ST} between pop. 1 & pop. 3	0.49	0.45	0.38	0.35
PairDiffs3vs4	Average no. of pairwise differences between pop. 3 & pop. 4	28.94	27.00	22.50	21.26
Fst3vs4	F_{ST} between pop. 3 & pop. 4	0.54	0.45	0.38	0.35

Table S3 Genus-specific primers developed for the study. CR, control region; cyt *b*, cytochrome *b*.

Name	Region	Primer seq. 5' - 3'	Fragment length w. primers (bp)
Lem_D1dF	CR	TATGTATAACGTACATTAAATTAT	129
Lem_D1cR	CR	GAATGTTTGATAGTCATATTCAT	
Lem_D2aF	CR	AGACATTAAAYTCTTTATCAAC	145
Lem_D2aR	CR	GCTGGGATAGACGTATGGAA	
Lem-CR-1F*	CR	ATTCCCCAAGCATATAAGCA	138
Lem-CR-1R*	CR	AAGATAACGCAGATATGTCTA	
Lem_C1aF	cyt *b*	CCTYCCAGCCCCATCAAAT	164
Lem_C1aR	cyt *b*	TAGTTTACGTCTCGGCAGAT	
Lem_C2aF	cyt *b*	GCAACAGCATTCTCATCAGT	165
Lem_C2aR	cyt *b*	TGTTTCAGGTTTCGATTATGTT	
Lem_C3aF	cyt *b*	CGRGGCGTTTACTACGGC	154
Lem_C3aR	cyt *b*	GATAGGAGGTTTGTAATTACTG	
Lem-cytb-1F*	cyt *b*	ATACATGCAAACGGAGCCTC	123
Lem-cytb-1R*	cyt *b*	AGCAAACAGTAGTACAATTCCT	

*Developed in Grenoble.

Table S4 Genetic diversity within modern, Holocene and Late Pleistocene sample regions. Number of successful samples (*n*), haplotypes (n_h), polymorphic sites (*S*), nucleotide diversity (π) and haplotype diversity (*H*) are shown for both the complete and partial data set respectively. Standard deviations are reported within square brackets. For the Holocene Scandinavian lemmings, the analyses have been made both including (i.) and excluding (e.) sample a6.

	520 bp					172 bp				
	n	n_h	*S*	π (s.d.)	*H* (s.d.)	*n*	n_h	*S*	π (s.d.)	*H* (s.d.)
Modern										
Scandinavia	17	10	13	0.0072 (0.0043)	0.93 (0.04)	17	9	9	0.0127 (0.0083)	0.92 (0.04)
NW Russia	10	6	13	0.0078 (0.0048)	0.84 (0.10)	10	6	9	0.0171 (0.0110)	0.84 (0.10)
Holocene										
Scandinavia, i.a6	-	-	-	-	-	8	5	15	0.0263 (0.0165)	0.79 (0.15)
Scandinavia, e.a6	-	-	-	-	-	7	4	3	0.0084 (0.0066)	0.71 (0.18)
Late Pleistocene										
England	6	4	8	0.0051 (0.0037)	0.80 (0.17)	6	3	7	0.0136 (0.0099)	0.60 (0.22)
Belgium	3	3	4	0.0051 (0.0046)	1.00 (0.27)	3	3	2	0.0078 (0.0080)	1.00 (0.27)
Germany	1	1	-	-	-	1	1	-	-	-
Poland	2	2	14	0.0269 (0.0279)	1.00 (0.50)	2	2	5	0.0291 (0.0318)	1.00 (0.50)
Russian plains	5	4	29	0.0300 (0.0189)	0.90 (0.16)	5	3	19	0.0605 (0.0389)	0.80 (0.16)
Ural mts	6	5	18	0.0147 (0.0093)	0.93 (0.12)	6	5	12	0.0291 (0.0190)	0.93 (0.12)
All glacial	*23*	*19*	*54*	*0.0275 (0.0143)*	*0.98 (0.02)*	*23*	*17*	*31*	*0.0553 (0.0294)*	*0.96 (0.03)*

Table S5 Phylogenetic tree node ages. Median ages and 95% highest posterior density (HPD) interval in thousands (k) of years before present, for the nodes shown in Fig. S2. The estimated times to the most recent common ancestor of all Scandinavian lemmings and the most closely related Late Pleistocene lemmings are shown in bold. Based on BEAST analyses of the complete data set, using a mutation rate of 8.9 %, 30 % and 50 % Myr^{-1}, respectively.

	8.9 % Myr^{-1}		30 % Myr^{-1}		50 % Myr^{-1}	
	Node age	95 % HPD	Node age	95 % HPD	Node age	95 % HPD
A	327 k	443 k - 233 k	120 k	155 k - 93 k	90 k	111 k - 73 k
B	241 k	330 k - 163 k	99 k	125 k - 78 k	78 k	93 k - 64 k
C	185 k	265 k - 123 k	69 k	90 k - 54 k	55 k	67 k - 47 k
D	88 k	130 k - 55 k	37 k	49 k - 27 k	29 k	37 k - 22 k
E	**64 k**	**95 k - 40 k**	**29 k**	**40 k - 20 k**	**23 k**	**30 k - 16 k**
F	50 k	81 k - 29 k	26 k	35 k - 19 k	22 k	28 k - 17 k
G	63 k	108 k - 33 k	23 k	37 k - 12 k	16 k	25 k - 9 k
H	46 k	71 k - 28 k	20 k	29 k - 12 k	14 k	21 k - 8 k

SI Figures

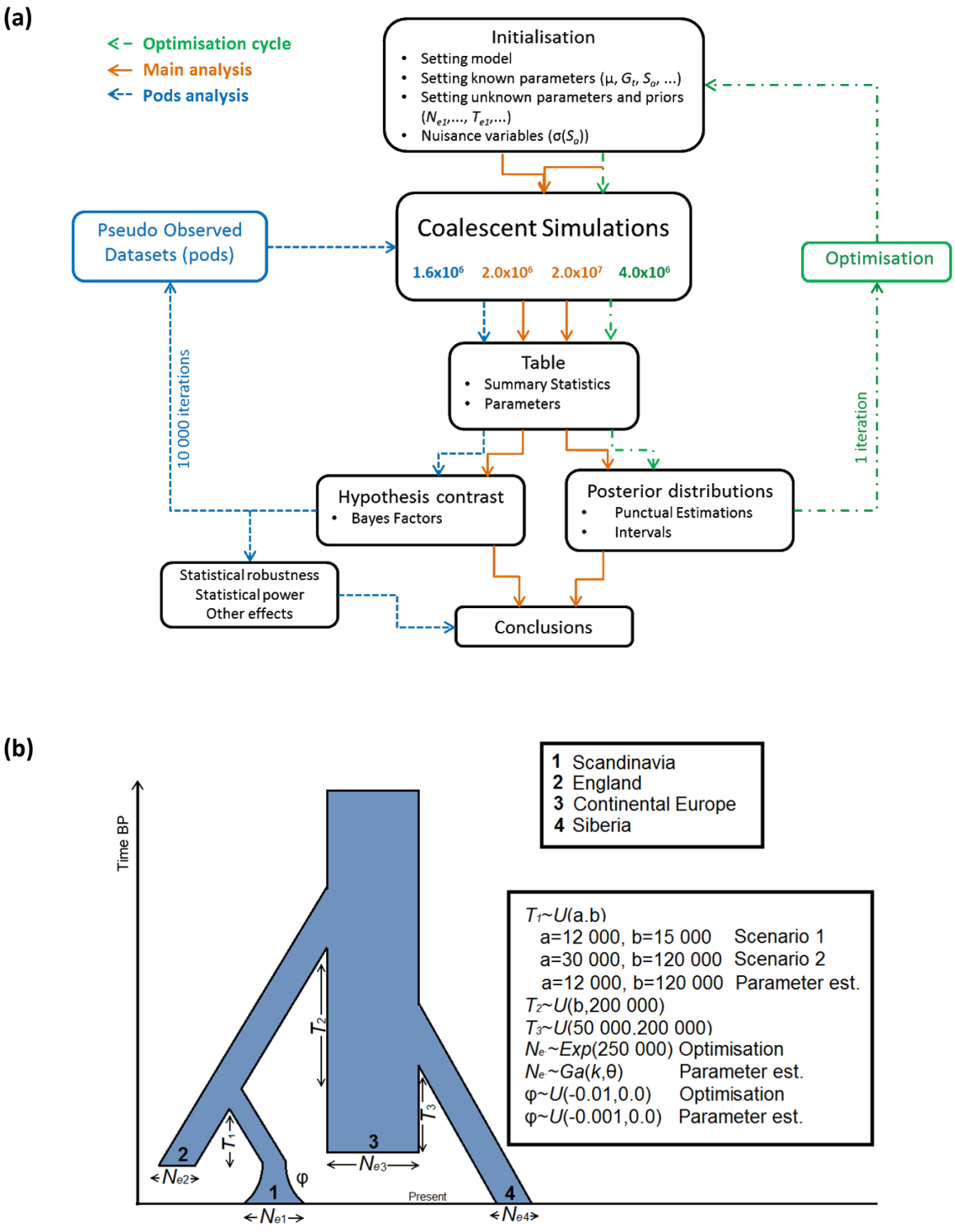

Fig. S1 Bayesian coalescent simulation methodology. (a) Schematic procedure followed in the analyses. (b) The simulated scenarios with different population split times, *T*, and effective population sizes, Ne.

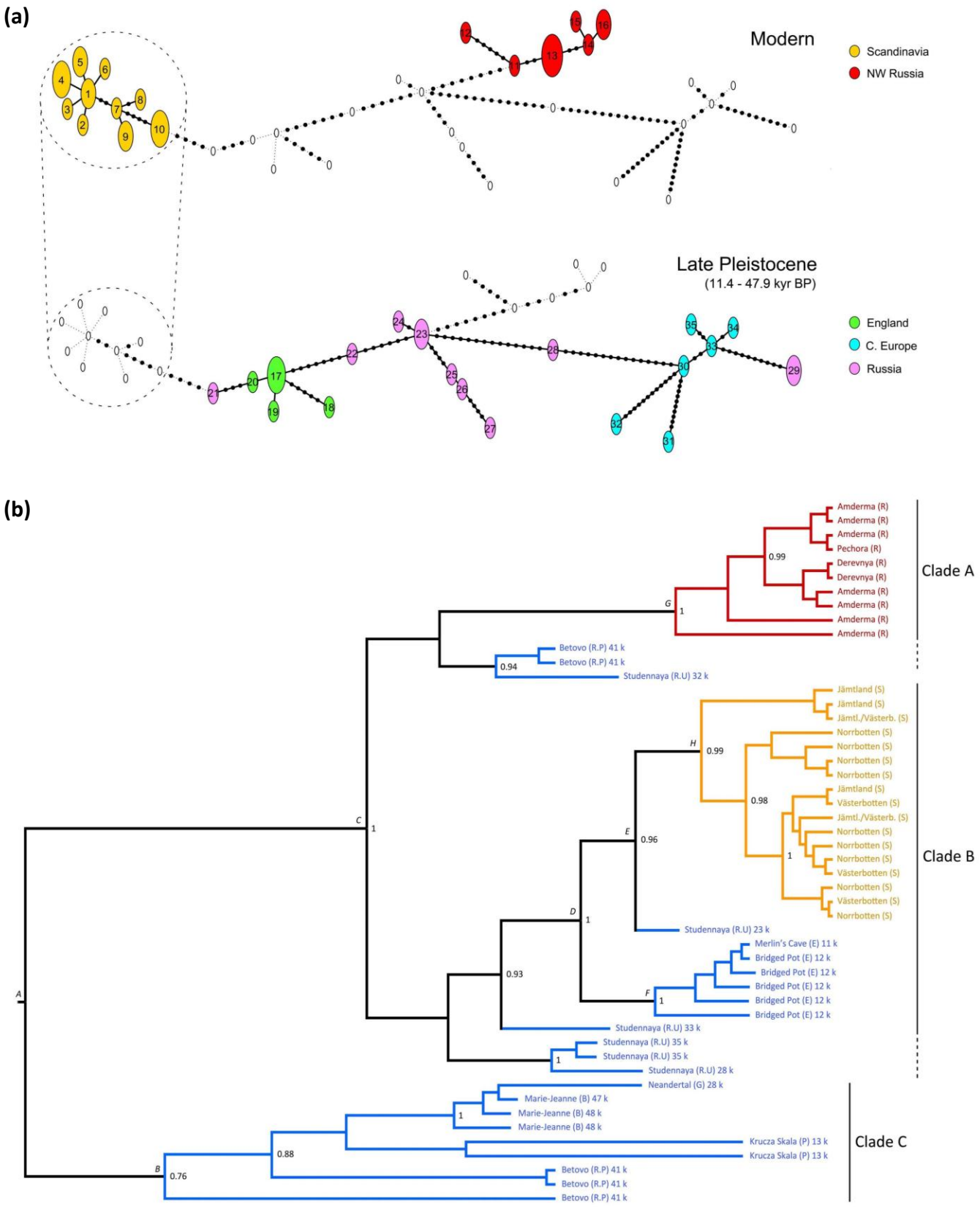

Fig. S2 Temporal statistical parsimony network (a) and Bayesian phylogeny constructed in BEAST (b). Based on the complete 520 bp data set, including only modern and Late Pleistocene samples, using a mutation rate of 30 % Myr^{-1}. Posterior probabilities of internal nodes above 0.75 are shown, with letters *A* to *H* referring to the estimated divergence times listed in Table S5. See Fig. 3 and Fig. 4 legends for more detailed information.

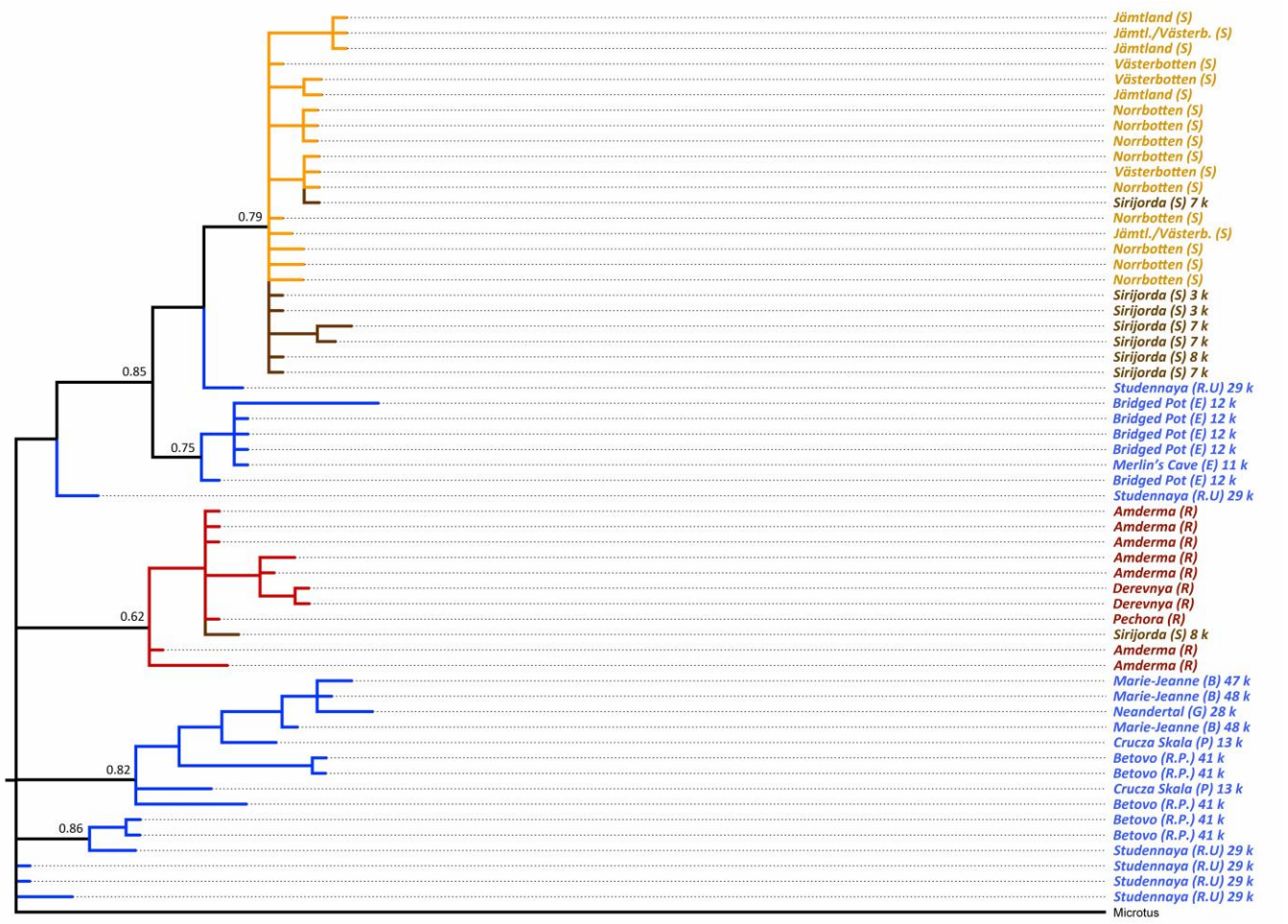

Fig. S3 Bayesian phylogeny constructed in MrBayes. The analysis is based on the partial data set, using the tundra vole *Microtus oeconomus* (Galbreath & Cook 2004) as an outgroup. Modern NW Russian *L. sibiricus* are shown in red, modern Scandinavian *L. lemmus* in yellow, early-mid Holocene Scandinavian samples in brown and Late Pleistocene European samples in blue. The ages of all ancient samples are shown in thousands (k) of years before present. S = Scandinavia; R = Russia; R.P = Russian plains; R.U = Russian Urals; P = Poland; G = Germany; B = Belgium; E = England. Probabilities of major internal nodes above 0.6 are shown.

11,7 %

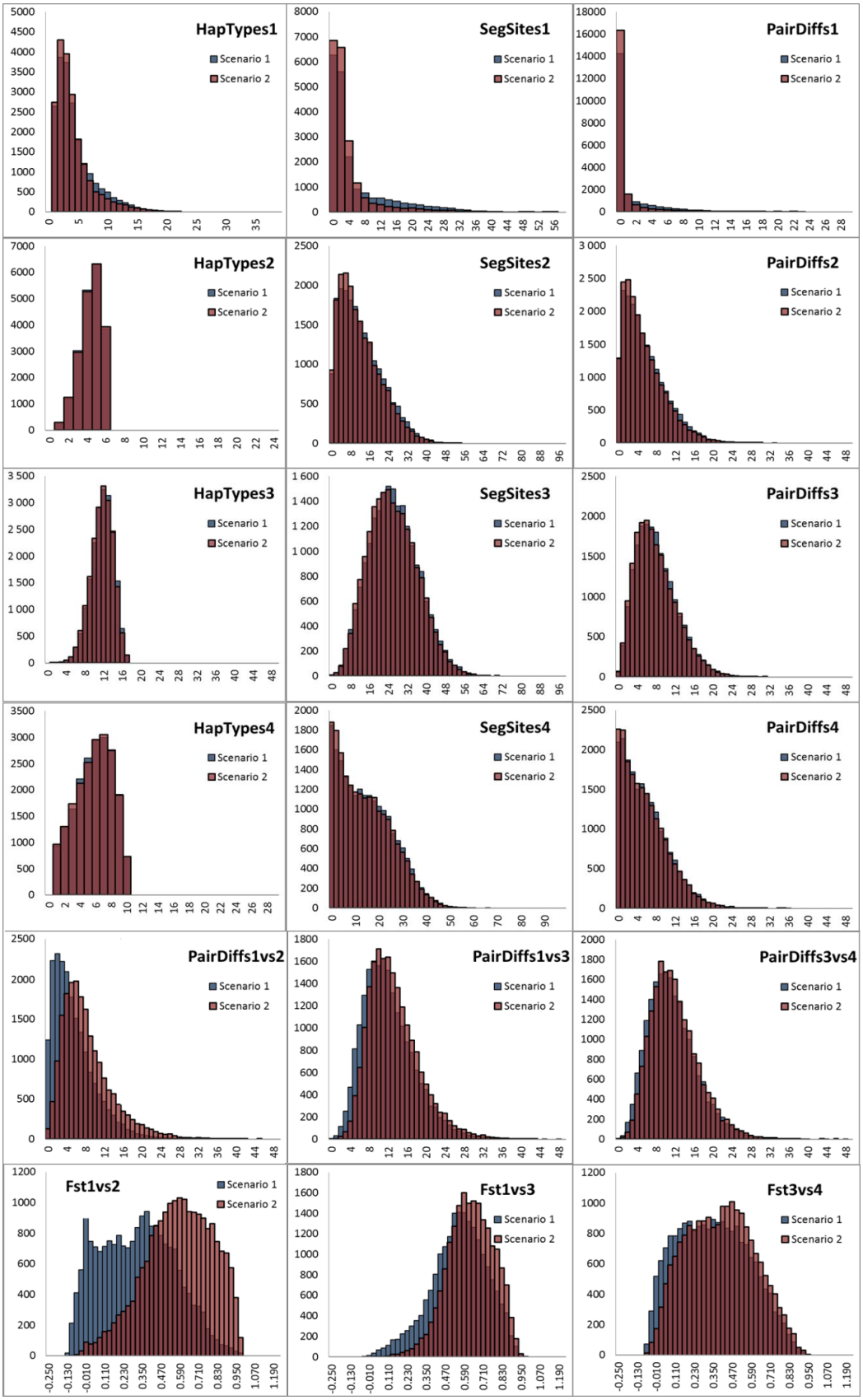
HapTypes1
SegSites1
PairDiffs1
HapTypes2
SegSites2
PairDiffs2
HapTypes3
SegSites3
PairDiffs3
HapTypes4
SegSites4
PairDiffs4
PairDiffs1vs2
PairDiffs1vs3
PairDiffs3vs4
Fst1vs2
Fst1vs3
Fst3vs4
Scenario 1
Scenario 2

30 %

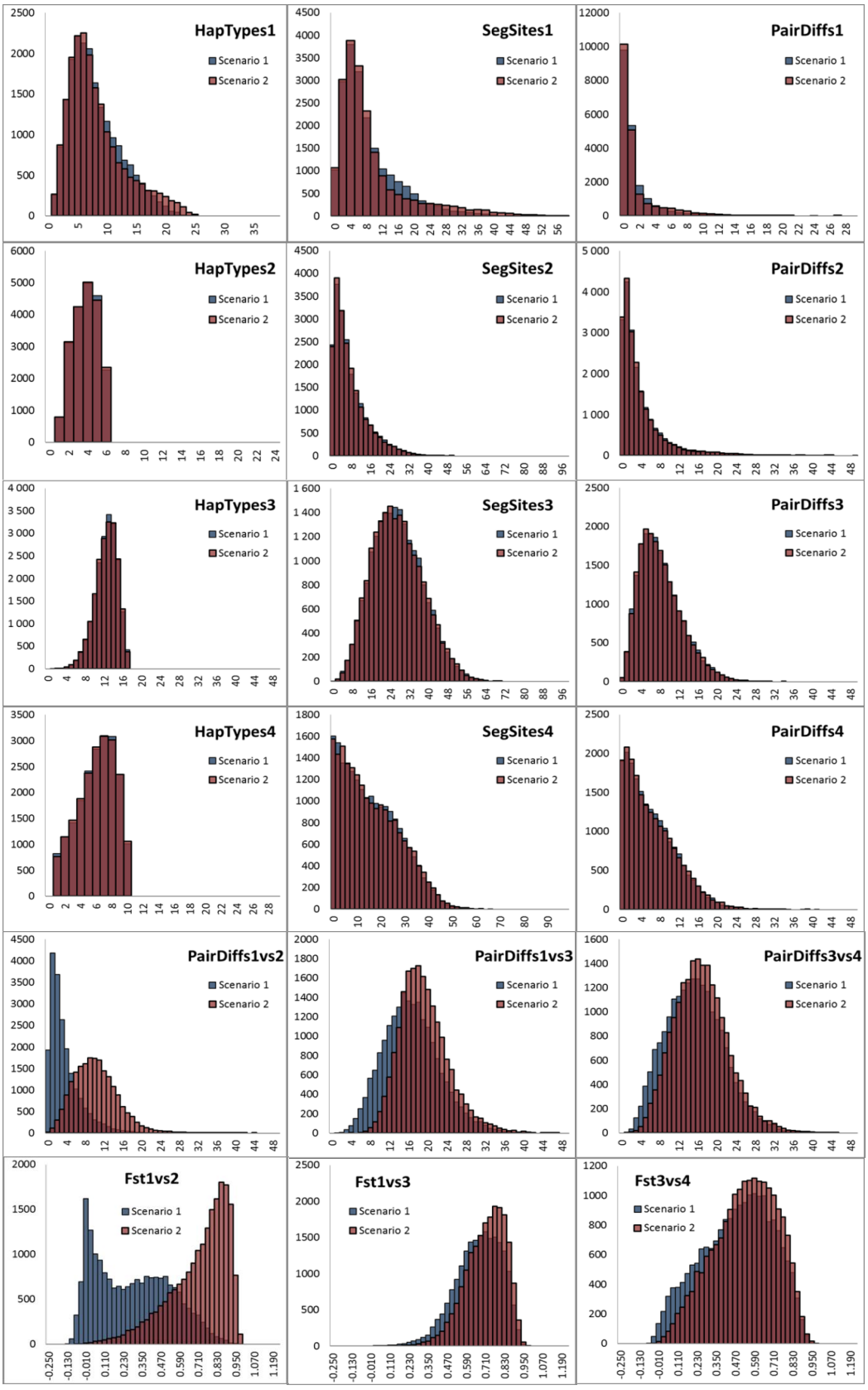
HapTypes1
SegSites1
PairDiffs1
HapTypes2
SegSites2
PairDiffs2
HapTypes3
SegSites3
PairDiffs3
HapTypes4
SegSites4
PairDiffs4
PairDiffs1vs2
PairDiffs1vs3
PairDiffs3vs4
Fst1vs2
Fst1vs3
Fst3vs4
Scenario 1
Scenario 2

50 %

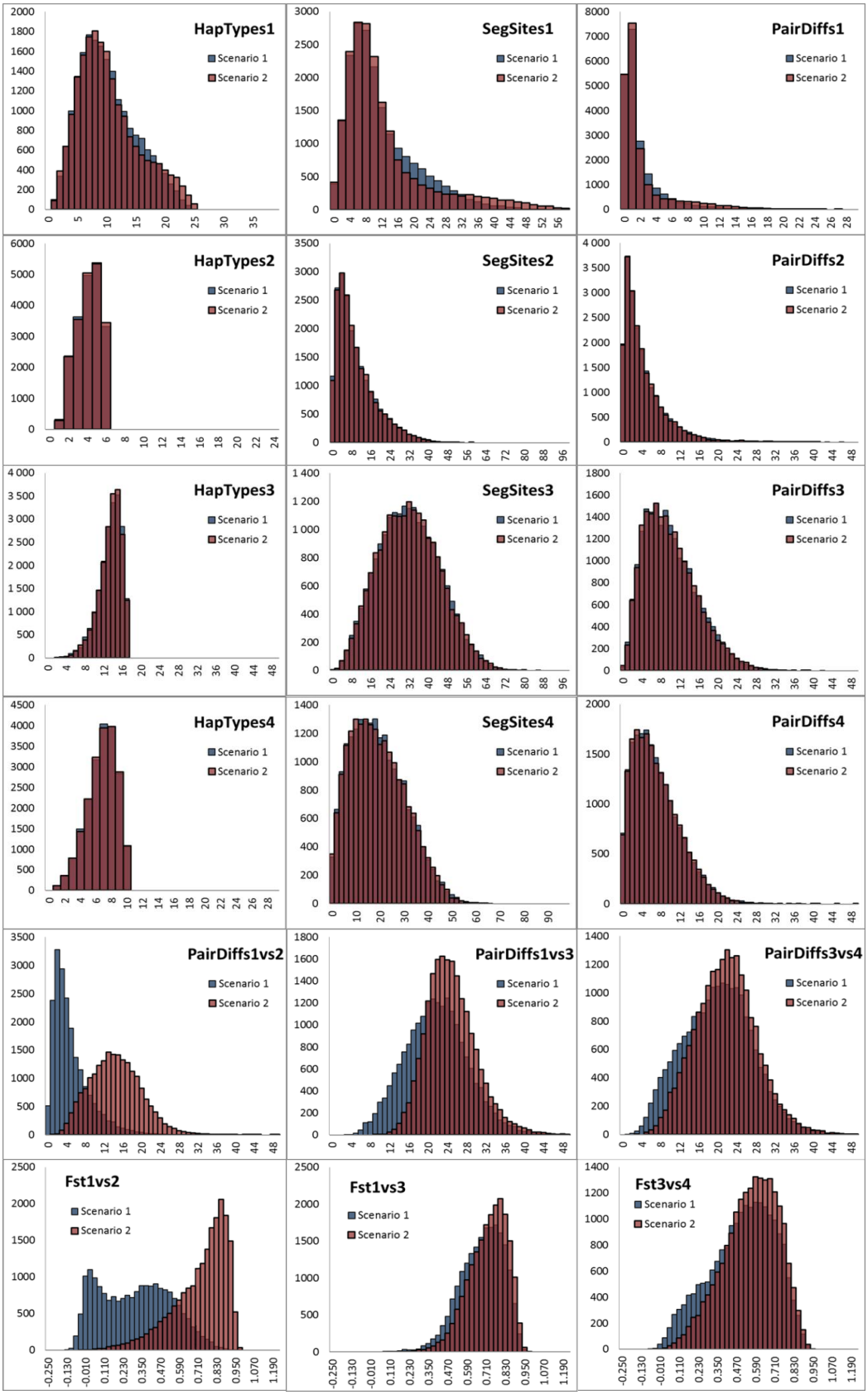

Fig. S4 Posterior distributions of the employed summary statistics for each scenario separately. Based on the Bayesian coalescent simulations of the partial data set, using three different mutation rates. No rejection has been applied.

11,7 %

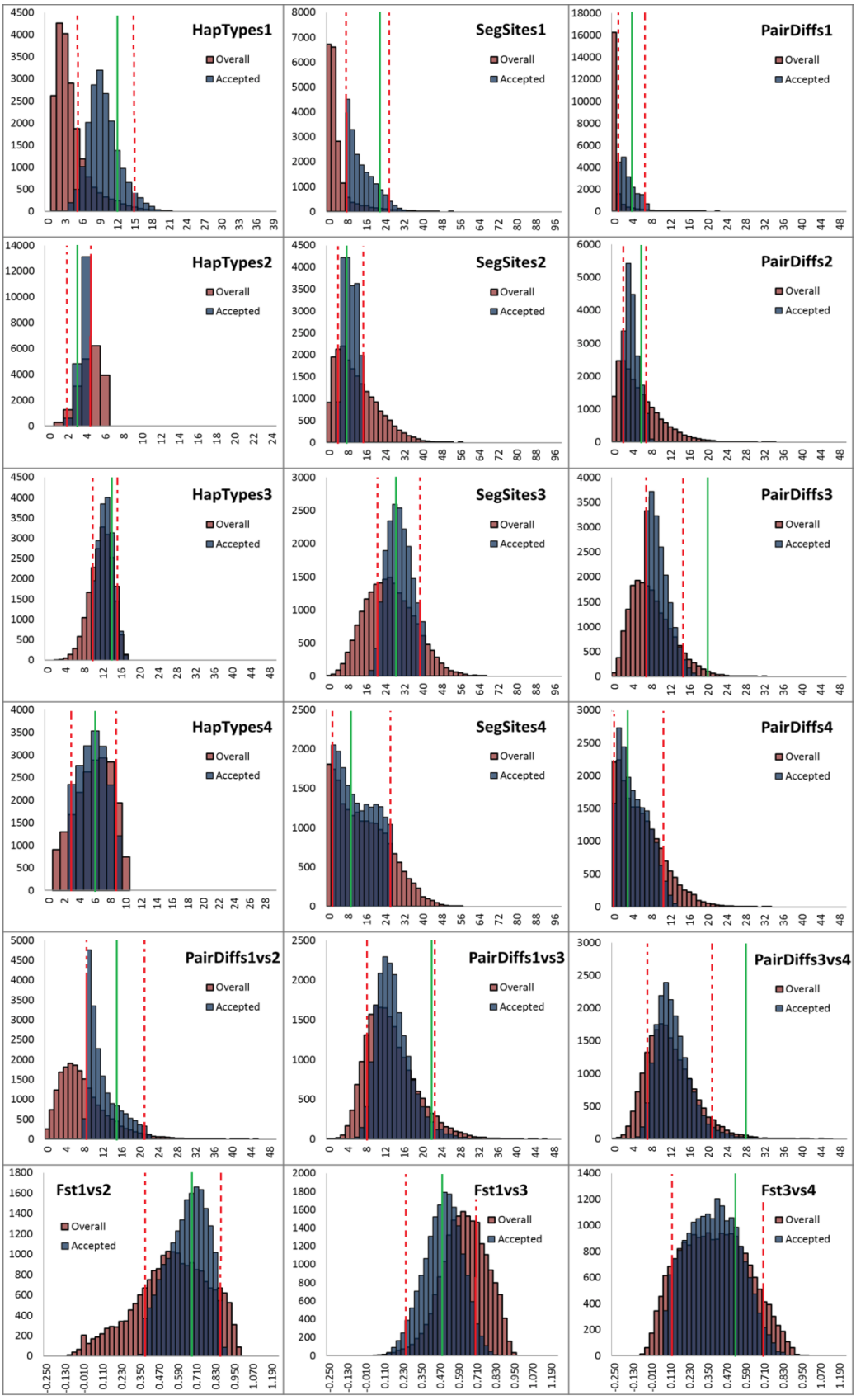
HapTypes1
SegSites1
PairDiffs1
HapTypes2
SegSites2
PairDiffs2
HapTypes3
SegSites3
PairDiffs3
HapTypes4
SegSites4
PairDiffs4
PairDiffs1vs2
PairDiffs1vs3
PairDiffs3vs4
Fst1vs2
Fst1vs3
Fst3vs4
Overall
Accepted

30 %

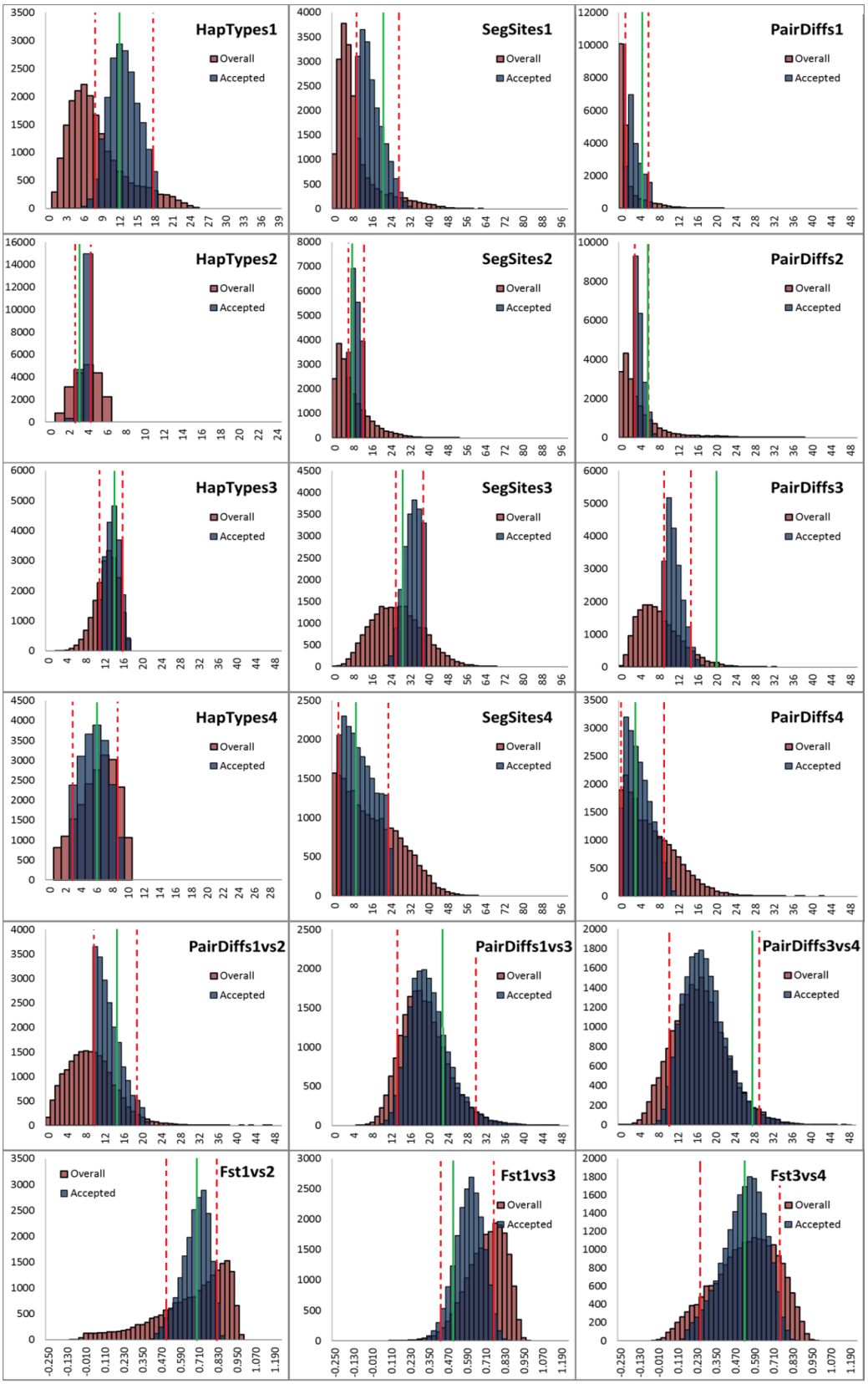
HapTypes1
SegSites1
PairDiffs1
HapTypes2
SegSites2
PairDiffs2
HapTypes3
SegSites3
PairDiffs3
HapTypes4
SegSites4
PairDiffs4
PairDiffs1vs2
PairDiffs1vs3
PairDiffs3vs4
Fst1vs2
Fst1vs3
Fst3vs4
Overall
Accepted

50 %

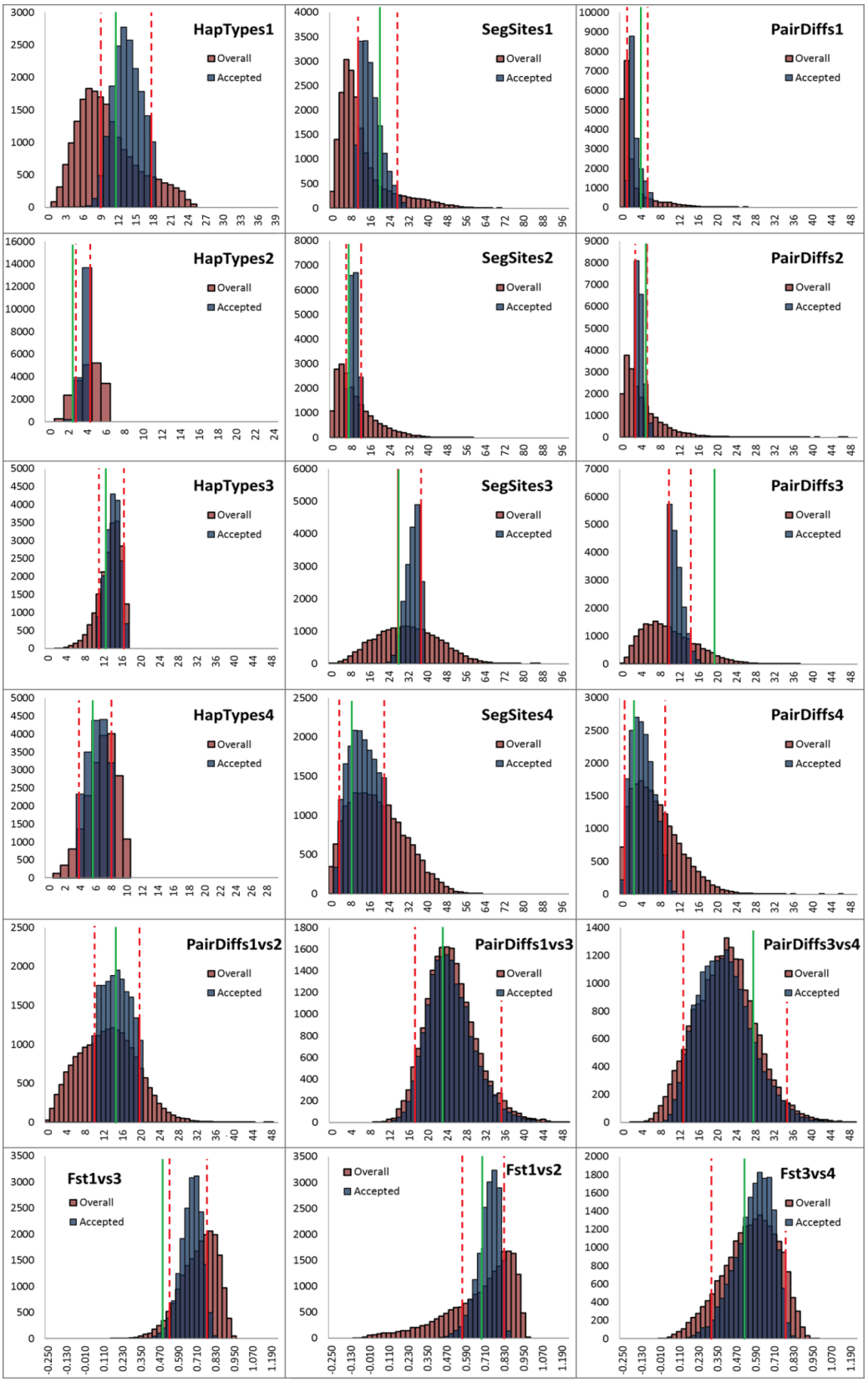

Fig. S5 Posterior distributions of the employed summary statistics for both scenarios combined. Based on the Bayesian coalescent simulations of the partial data, using three different mutation rates. The whole set of simulations is shown in red, and the accepted ones in blue. Red dashed lines show the boundaries of the 95% C.I. of the accepted simulations, while the green solid line indicates our observed values.

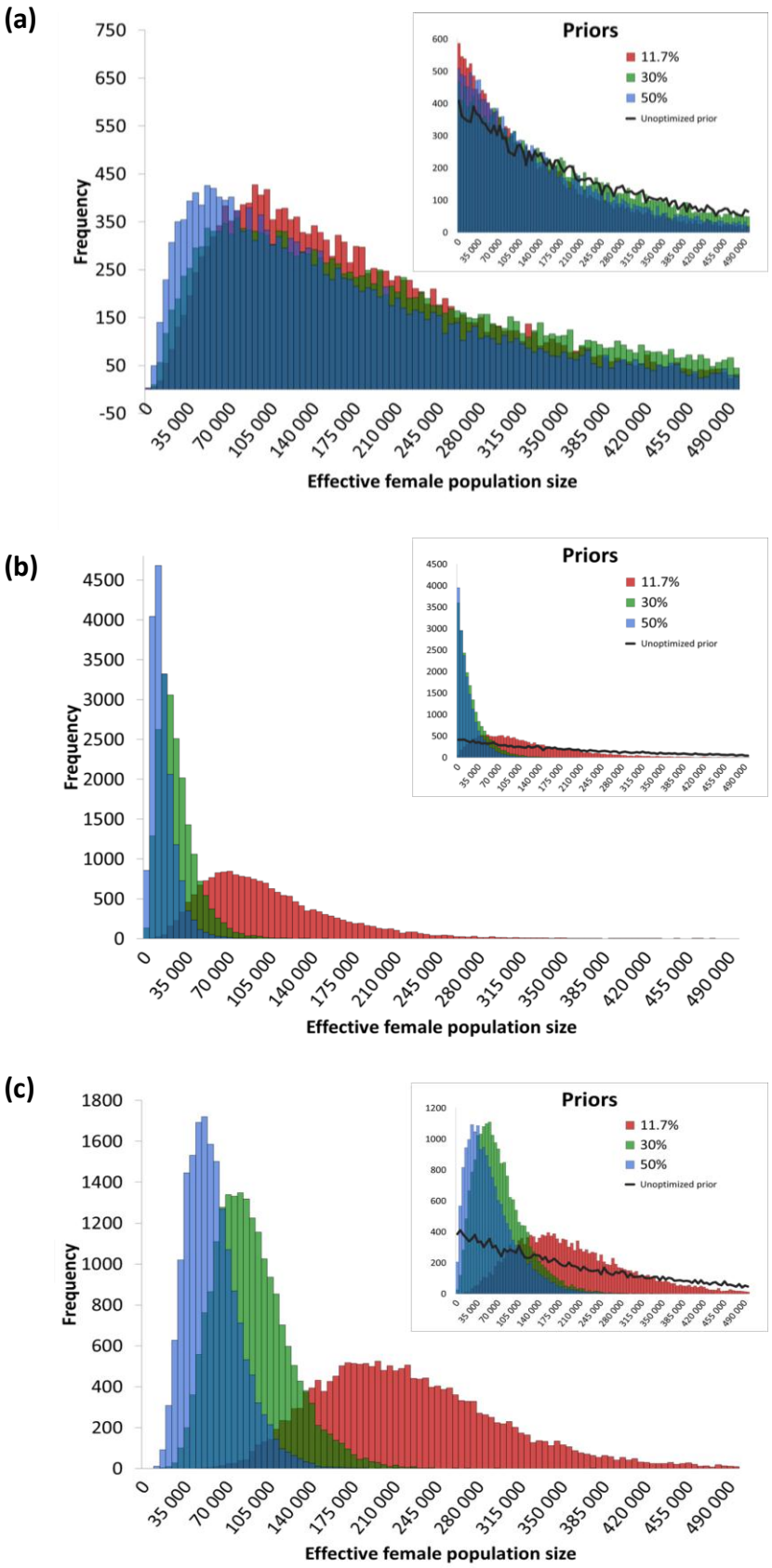

Fig. S6 Posterior probability distributions for different effective population sizes. Based on the Bayesian coalescent simulations of the partial data set, using three different mutation rates. (a) Scandinavian lemmings. (b) Glacial English lemmings. (c) Glacial continental European lemmings.

SI References

Abramson NI, Smirnov NG, Tikhonova EP (2004) Morphological studies on collared lemmings (Rodentia, Arvicolidae, *Dicrostonyx*) from Bolshevik Island of the Severnaya Zemlya Archipelago, with notes on evolution and taxonomic position. *Russian Journal of Theriology*, **3**, 63-70.

Anderson CNK, Ramakrishnan U, Chan YL, Hadly EA (2005) Serial SimCoal: A population genetics model for data from multiple populations and points in time. *Bioinformatics*, **21**, 1733-1734.

Beaumont MA, Zhang WY, Balding DJ (2002) Approximate Bayesian computation in population genetics. *Genetics*, **162**, 2025 - 2035.

Bertorelle G, Benazzo A, Mona S (2010) ABC as a flexible framework to estimate demography over space and time: some cons, many pros. *Molecular Ecology*, **19**, 2609-2625.

Bochenski Z, Tomek T (2004) Bird remains from a rock-shelter in Krucza Skala (Central Poland). *Acta zoologica cracoviensia*, **47**, 27-47.

Excoffier L, Novembre J, Schneider S (2000) SIMCOAL: A general coalescent program for the simulation of molecular data in interconnected populations with arbitrary demography. *Journal of Heredity*, **91**, 506-509.

Fernández H, Hughes S, Vigne J-D, *et al.* (2006) Divergent mtDNA lineages of goats in an Early Neolithic site, far from the initial domestication areas. *Proceedings of the National Academy of Sciences*, **103**, 15375-15379.

Galbreath KE, Cook JA (2004) Genetic consequences of Pleistocene glaciations for the tundra vole (Microtus oeconomus) in Beringia. *Molecular Ecology*, **13**, 135-148.

Lopes JS, Balding D, Beaumont MA (2009) PopABC: a program to infer historical demographic parameters. *Bioinformatics*, **25**, 2747 - 2749.

Lopes JS, Beaumont MA (2010) ABC: A useful Bayesian tool for the analysis of population data. *Infection, Genetics and Evolution*, **10**, 825-832.

Ramsey CB, Higham TFG, Owen DC, Pike AWG, Hedges REM (2002) Radiocarbon dates from the Oxford AMS System: archaeometry datelist 31. *Archaeometry*, **44**, 1-149.

Yang DY, Eng B, Waye JS, Dudar JC, Saunders SR (1998) Improved DNA extraction from ancient bones using silica-based spin columns. *American Journal of Physical Anthropology*, **105**, 539-543.

Østbye E, Lauritzen S-E, Moe D, Østbye K (2006) Vertebrate remains in Holocene limestone cave sediments: faunal succession in the Sirijorda Cave, northern Norway. *Boreas*, **35**, 142-158.